

Received 16 February 2024, accepted 7 March 2024, date of publication 11 March 2024, date of current version 18 March 2024.

Digital Object Identifier 10.1109/ACCESS.2024.3375927

RESEARCH ARTICLE

Multiscale Modeling of 3-D Electromagnetic Fields With Magnetization Dynamics

YUTA ITO, TAKUMI YASUDA¹, SEIYA KISHIMOTO¹, (Member, IEEE),
KATSUJI NAKAGAWA, (Member, IEEE), AND
SHINICHIRO OHNUKI¹, (Member, IEEE)

College of Science and Technology, Nihon University, Tokyo 102-8275, Japan

Corresponding author: Shinichiro Ohnuki (ohnuki.shinichiro@nihon-u.ac.jp)

This work was supported in part by the Japan Society for the Promotion of Science (JSPS) KAKENHI under Grant JP17K06401 and Grant JP23K03961.

ABSTRACT Multiphysics simulation of Maxwell's and Landau–Lifshitz–Gilbert equations are performed to solve electromagnetic fields by considering the dynamics of magnetization. These equations are discretized, and the time-domain responses are computed using a finite-difference time-domain scheme. This study focuses on the acceleration of multiphysics simulations in terms of the multiscale modeling of the interaction between electromagnetic fields and magnetization. A nanoscale magnetic film is conducted to develop a method for measuring the magnetic properties using the near field of the magnetic film.

INDEX TERMS Finite-difference time-domain (FDTD) scheme, Landau–Lifshitz–Gilbert (LLG) equation, multiphysics simulation, multiscale modeling.

I. INTRODUCTION

Recently, the development of devices based on spin dynamics and studies on the magnetic properties of materials have been conducted in the field of magnetic materials [1], [2], [3], [4], [5], [6], [7], [8]. In the electromagnetic field analysis of magnetic materials, magnetic permeability is expressed using a constant value, tensor with dispersion, frequency-independent tensor with dispersion, or by solving the Landau–Lifshitz–Gilbert (LLG) equation [2], [3], [4], [5], [6]. The permeability tensor is formulated under the assumption that the magnetization in the magnetic material is saturated in a certain direction and constantly moves along a fixed rotation axis [9]. The LLG equation can be used to perform multiphysics simulations of magnetization and nonlinear electromagnetic fields. Magnetization has been incorporated into Maxwell's equation under the small-signal approximation [10], [11], [12], [13], [14], [15], [16], [17]. However, the LLG equation was not solved directly; thus, the dynamics of magnetization could not be considered.

References [18] and [19] showed that the dynamics of magnetization can be treated by solving the LLG equation

The associate editor coordinating the review of this manuscript and approving it for publication was Shashikant Patil¹.

using an implicit and iterative solver. Maxwell's equation and the LLG equation have been solved using the finite-difference time-domain (FDTD) scheme to analyze the electromagnetic problems of magnetic materials. The simulation method reported in [18] and [19], which is an electromagnetic analysis that considers the dynamics of magnetization, is useful for analyzing spin waves and designing related devices. To simulate spin dynamics, it is crucial to solve the LLG equations, including the exchange interaction and angular momentum. For research on spin oscillators in the terahertz range [7], [8], it is necessary to consider the exchange interaction, which is a quantum mechanical effect between magnetizations, and the interaction between electromagnetic fields and magnetizations.

The conventional method proposed in [18] and [19] can simultaneously solve the LLG and Maxwell's equations. The electromagnetic fields and magnetization were discretized using a standard Yee cell [9]. The effects of magnetization dynamics are incorporated into the electromagnetic fields. Here, the LLG equation is solved implicitly. Thus, the stability conditions need not be considered when solving the LLG equation. The simulation is numerically stable if the numerical stability conditions for solving Maxwell's equations are satisfied. As the time step size of explicit FDTD depends on

the space step size of the Yee cell, the computational time increases for a more accurate simulation [9]. Furthermore, the magnetization needs to be modeled in sub-nano-meter size for the analysis considering the exchange interaction, and the finite difference should be implemented to obtain highly accurate results. As a result of the complete expression of the effects of the exchange interaction, the magnetization space step size must become extremely small for detailed modeling in the sub-nanometer size. However, because the resonance phenomenon of spin waves occurs in the microwave band, the wavelength of the electromagnetic field to be analyzed in free space ranges from several millimeters to centimeters. Simultaneous coupling analysis between the exchange interaction and the electromagnetic field in the microwave band becomes a large-scale problem that requires 10^6 to 10^7 divisions for one wavelength.

In this study, a novel multiscale model was applied for the fast computation of electromagnetic analysis with magnetics dynamics. The computation time for analyzing the interaction between the electromagnetic field and magnetization can be reduced using multiscale modeling. Several studies [20], [21] have been conducted on multiphysics simulations, and the multiscale model proposed in this study is applicable to various multiphysics simulations. The space step size of the electromagnetic field and that of the magnetizations were considered variables. It reduces the number of time steps required to obtain accurate results because the space step size of electromagnetic fields larger than that of magnetization can be selected. Furthermore, as an application of this method, a nanoscale magnetic film is analyzed in this study. Moreover, the magnetic properties can be measured from the magnetic field near the magnetic film.

II. FORMULATION

A. MULTIPHYSICS SIMULATION FOR ELECTROMAGNETIC FIELDS AND MAGNETIZATION DYNAMICS

Magnetic field analysis, considering the dynamics of magnetization, was performed using the FDTD scheme with the Yee cell, as shown in Fig. 1 [7], [18], [19]. In this case, the arrangement of the magnetic field is expressed around the magnetization placed at the lattice points in the Yee cell. The electromagnetic field and magnetization dynamics were calculated from (1) (Maxwell's equation) and (2) (the LLG equation) [22], respectively.

$$\nabla \times \mathbf{H}_M = \mathbf{J} + \varepsilon \frac{\partial \mathbf{E}}{\partial t},$$

$$\nabla \times \mathbf{E} = -\frac{\partial \mathbf{B}}{\partial t} \quad (1)$$

$$\frac{d\mathbf{M}_L}{dt} = -\gamma \mathbf{M}_L \times \mathbf{H}_{eff} + \frac{\alpha}{M_s} \mathbf{M}_L \times \frac{d\mathbf{M}_L}{dt}. \quad (2)$$

Here, \mathbf{H}_M denotes the magnetic fields to update the electric field, \mathbf{B} denotes the magnetic flux density, \mathbf{E} indicates the electric field, \mathbf{J} denotes the current density, ε signifies the permittivity, μ_0 symbolizes the permeability for free space, and \mathbf{M}_L indicates the magnetization obtained. In solving the

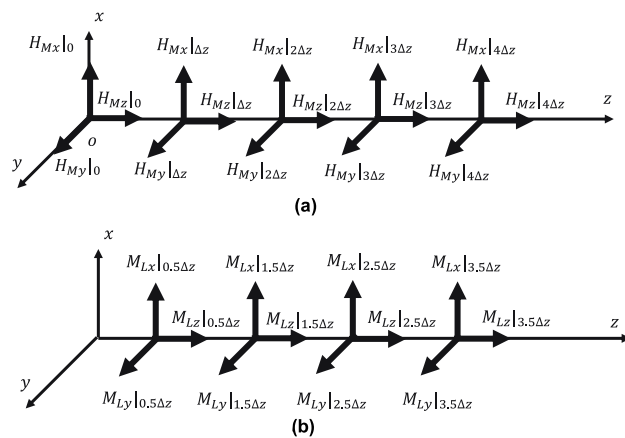


FIGURE 1. Yee cell for multiphysics simulation. (a) Position of magnetic field vector components and (b) magnetization vector components.

LLG equation, γ is the gyromagnetic ratio, α is the damping constant, and M_s indicates the saturation magnetization. The effective magnetic field \mathbf{H}_{eff} indicates the magnetic field applied to create magnetization, which is expressed using the following equation:

$$\mathbf{H}_{eff} = \mathbf{H}_L + \mathbf{H}_B. \quad (3)$$

Here, \mathbf{H}_L denotes the externally time-varying magnetic field applied to the magnetization and represents the component of the magnetic field used to solve the LLG equation. \mathbf{H}_B indicates the externally given static magnetic field to saturate the magnetization. The external magnetic field is obtained by solving Maxwell's equations with FDTD. For example, an incident electromagnetic wave applied to a magnetic material or a magnetic field generated by magnetization elsewhere corresponds to an external magnetic field.

In these equations, the dynamics of the electromagnetic field and magnetization are coupled using the following equations: The magnetic field \mathbf{H}_M was obtained using the following equation:

$$\mathbf{H}_M = \frac{\mathbf{B}}{\mu_0} - \mathbf{M}_M, \quad (4)$$

where \mathbf{M}_M denotes the magnetization calculated from the LLG equation and converted to Maxwell's equations.

The interaction between the electromagnetic field and magnetization dynamics can be calculated from these equations.

In the FDTD method, the electromagnetic field and magnetization are discretized using a Yee cell. Maxwell's equation (1) was applied to the finite difference and solved using an explicit scheme.

Magnetization was calculated using the central differences in (2). The updated equation at time step n is given by:

$$\mathbf{M}_L^n = \mathbf{M}_L^{n-1/2} - \mathbf{M}_L^n \times \left(\frac{|\gamma| \Delta t}{2} \mathbf{H}_{eff}^n(\mathbf{M}_L^n) + \frac{\alpha}{M_s} \mathbf{M}_L^{n-1/2} \right). \quad (5)$$

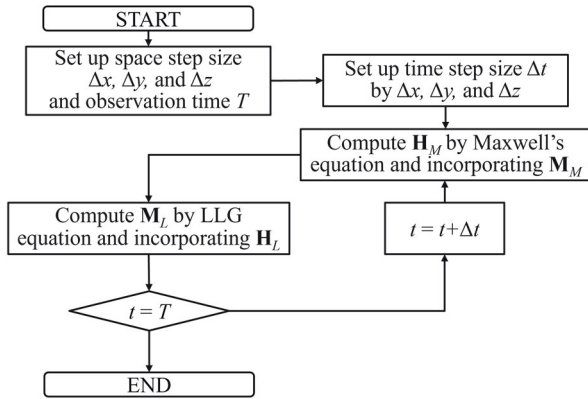


FIGURE 2. Flowchart of multiphysics simulation for electromagnetic fields and dynamics of magnetization.

However, these schemes cannot be applied explicitly to (5). Thus, implicit and iterative numerical schemes were applied to solve (5), as shown in [18], [20], and [23]. To obtain $[\mathbf{M}^n]^r$, which is the magnetization for iteration number r , the updated LLG equation can be rewritten as

$$[\mathbf{M}_L^n]^r = \frac{\mathbf{M}_L^{n-1/2} + \left(\boldsymbol{\beta} \cdot \mathbf{M}_L^{n-1/2}\right) \boldsymbol{\beta} - \boldsymbol{\beta} \times \mathbf{M}_L^{n-1/2}}{1 + |\boldsymbol{\beta}|^2} \quad (6)$$

$$\boldsymbol{\beta} = -\left(\frac{|\gamma|\Delta t}{2} \mathbf{H}_{eff}^n([\mathbf{M}_L^n]^{r-1}) + \frac{\alpha}{M_s} \mathbf{M}_L^{n-1/2}\right) \quad (7)$$

Equation (6) is iteratively solved until the convergence criterion $|\overline{[\mathbf{M}_L^n]^r} - \overline{[\mathbf{M}_L^n]^{r-1}}| \leq 10^{-15}$ is met to achieve machine precision, where $\overline{[\mathbf{M}_L^n]^r}$ indicates the average of the magnetization of the neighboring iterations by one cell around the magnetization to be found for the r -th time. Here, a numerical accuracy equivalent to machine precision is selected. Multiphysics analysis that couples the time evolution of the electromagnetic field and magnetization requires satisfying the numerical stability conditions for both the electromagnetic field and magnetization. The time evolution of magnetization can be computed with unconditional stability using the implicit and iterative method. Therefore, the electromagnetic field and magnetization can be computed considering only the stability conditions of the electromagnetic field.

Fig. 2 shows a flowchart of the multiphysics simulation of the electromagnetic fields and dynamics of magnetization. The magnetic flux density \mathbf{B} and electric fields \mathbf{E} were computed using an explicit FDTD scheme. The magnetic field \mathbf{H}_M is obtained using (4) and magnetization vector \mathbf{M}_M . Since the discretization sizes of the electromagnetic field and magnetization are the same, the magnetization \mathbf{M}_L obtained by solving the LLG equation is substituted into \mathbf{M}_M . The magnetization vectors were obtained via the iterative method using the effective magnetic field \mathbf{H}_{eff} , which includes the magnetic field calculated from Maxwell's equation, \mathbf{H}_L . \mathbf{H}_M obtained from (4) is substituted into \mathbf{H}_L . Moreover, the time

evolution of the magnetization can be updated stably using an iterative method. In this multiphysics simulation, the LLG equations were solved using the iterative method, which is an implicit solution method, and Maxwell's equations were solved using the FDTD method, which is an explicit solution method. Therefore, the time-step size is limited by the FDTD method.

B. MULTISCALE MODELING

In the FDTD scheme used in this method, an upper limit to the time step size Δt is imposed. The speed at which information propagates is higher than that at which waves propagate in actual phenomena. The stability condition for this method is called the Courant–Friedrich–Levy condition [7]. For three-dimensional (3D) propagation problems, we will be dealing with the limited time step size as follows,

$$\Delta t \leq \frac{1}{c \cdot \sqrt{\left(\frac{1}{\Delta x}\right)^2 + \left(\frac{1}{\Delta y}\right)^2 + \left(\frac{1}{\Delta z}\right)^2}}. \quad (8)$$

As the space step size $\Delta x, \Delta y, \Delta z$ decreases, Δt decreases, whereas the computational cost increases. However, because the LLG equation is solved using implicit and iterative numerical schemes, a limit does not exist for the time step size based on the cell size. Furthermore, in magnetization analysis, the target object is often small compared to the wavelength of the electromagnetic wave. Therefore, the spatial step size required for magnetization analysis is smaller compared to the spatial step size required for magnetic field analysis. Therefore, the space step size of the electromagnetic field can be set larger than the space step size of magnetization dynamics. The proposed method leverages this fact and sets the space step size of the electromagnetic field larger than the space step size of the magnetization dynamics to reduce the computation time.

Fig. 3 shows the positions of the magnetic field vector components and the magnetization vector for multiscale modeling applied in the z -direction. The ratio of the space step size of the magnetic fields to the magnetization, k , is 2. The grid used for solving the LLG equation is the same as that used in a previous multiphysics simulation; k is given as

$$k = \frac{\text{Space step size of electromagnetic field}}{\text{Space step size of magnetization dynamics}} \quad (9)$$

In the conventional method or $k = 1$, since the discrete size of the electromagnetic field and magnetization are the same, the magnetization \mathbf{M}_L obtained from the LLG equation is used as the magnetization \mathbf{M}_M for updating the electromagnetic field. Therefore, $\mathbf{M}_M = \mathbf{M}_L$ and $\mathbf{H}_M = \mathbf{H}_L$ are selected. Our proposed multiscale method is designed to set the cell size for solving Maxwell's equations larger than that for solving the LLG equation. In this case, $\mathbf{M}_M = \mathbf{M}_L$ and $\mathbf{H}_M = \mathbf{H}_L$ cannot be selected.

The magnetic field \mathbf{H}_L is required to update magnetization \mathbf{M}_L in (5). As the cell size for solving Maxwell's and LLG equations is different, $\mathbf{H}_M = \mathbf{H}_L$ could not be selected. \mathbf{H}_L is

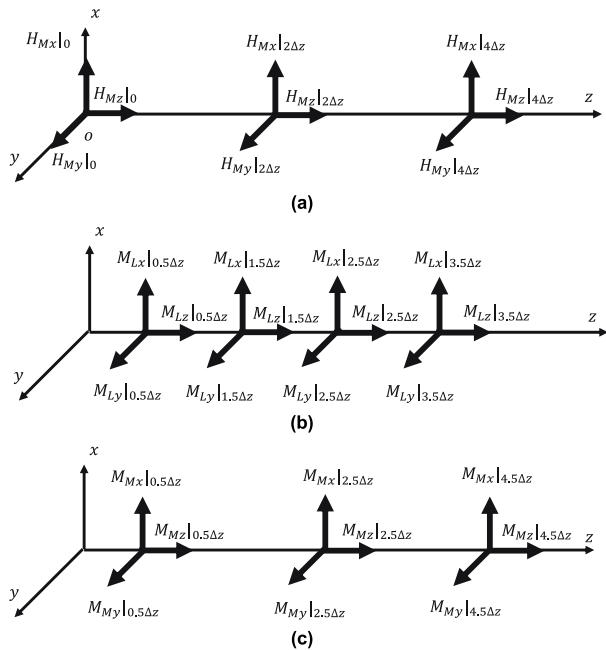


FIGURE 3. Discretization for multiphysics simulation. (a) Position of electromagnetic field vector components for $k = 2$, (b) Position of magnetization vector for solving the LLG equation, and (c) magnetization vector for solving Maxwell's equation.

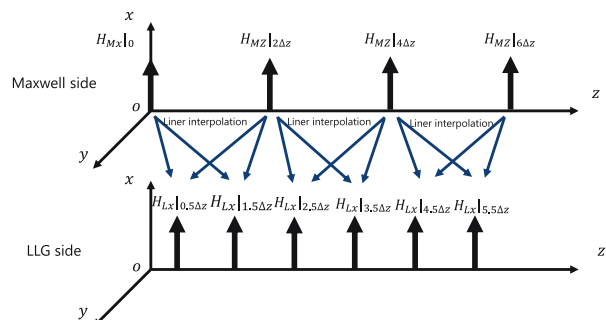


FIGURE 4. Linear approximation for computing the magnetic fields for solving LLG equation.

obtained by linear interpolation from the magnetic field \mathbf{H}_M , which is obtained by solving Maxwell's equation, as shown in the following equation and Fig. 4.

$$\begin{aligned} \mathbf{H}_L(kn\Delta z + l\Delta z) &= \mathbf{H}_M(kn\Delta z) + \frac{l\Delta z}{k\Delta z}(\mathbf{H}_M(kn\Delta z + k\Delta z) - \mathbf{H}_M(kn\Delta z)) \end{aligned} \quad (10)$$

Here, $0 \leq l \leq k$.

On the other hand, the magnetic field \mathbf{H}_M obtained by solving Maxwell's equations is computed by the magnetization \mathbf{M}_M as (4). Here, $\mathbf{M}_M = \mathbf{M}_L$ can be selected if the cells for solving Maxwell's equations and the cells for solving the LLG equations are identical. However, if the cell sizes for solving the LLG and Maxwell's equations are different, $\mathbf{M}_M = \mathbf{M}_L$ cannot be selected. To obtain the magnetization

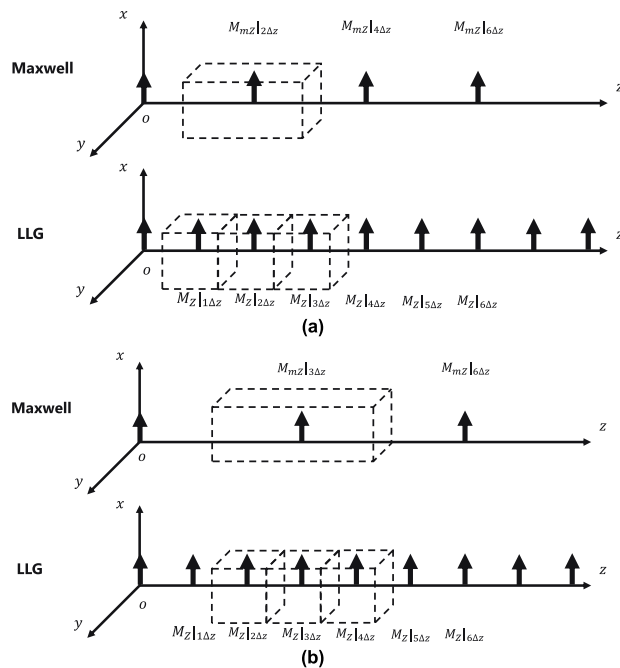


FIGURE 5. Discretization for multiphysics simulation for multiscale method. (a) $k = 2$ and (b) $k = 3$.

\mathbf{M}_M for solving Maxwell's equations, the magnetizations \mathbf{M}_L obtained by solving the LLG equation are weighted and summed as

$$\mathbf{M}_M(kn\Delta z) = \sum_{i=-L}^L W_i \mathbf{M}_L((kn+i)\Delta z), \quad (11)$$

where W_i denotes the weight and L corresponds to the number of the \mathbf{M}_L to determine \mathbf{M}_M .

We consider the extent to which the cells for solving Maxwell's equations cover the cells for solving the LLG equations. Fig. 5 illustrates the discretization of the multiphysics simulation using the multiscale method. (a) $k = 2$ and (b) $k = 3$. When k is an even number, the cell end for solving Maxwell's equations is placed at the center of the cell to solve the LLG equations. As half of the cell for solving the LLG equation is contained in the cell to solve Maxwell's equations, the magnetization at the end of the cell for solving Maxwell's equations must be added with a weight of $1/2$, which is determined in numerical experiments. Therefore, when k is an even number, \mathbf{M}_M for solving Maxwell's equations is obtained using the following equation:

$$\begin{aligned} \mathbf{M}_M(kn\Delta z) &= \sum_{i=1-\frac{k}{2}}^{\frac{k}{2}-1} \mathbf{M}_L((kn+i)\Delta z) \\ &\quad + \frac{1}{2}(\mathbf{M}_L(kn\Delta z + k\Delta z/2) + \mathbf{M}_L(kn\Delta z - k\Delta z/2)) \end{aligned} \quad (12)$$

Fig. 6 shows a flowchart of the multiscale modeling. The magnetic field was computed using the magnetization vector

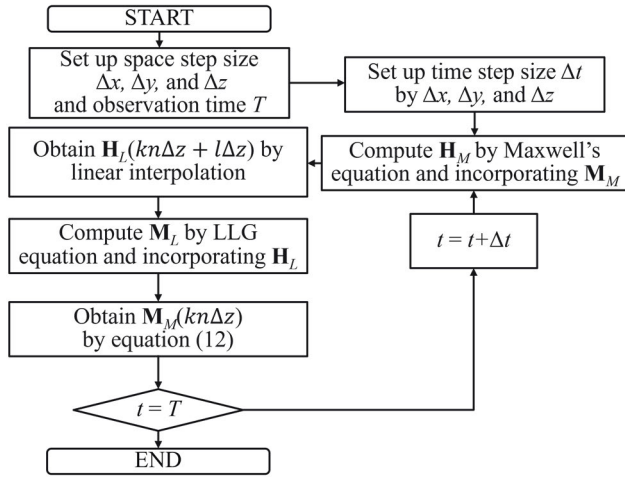


FIGURE 6. Flowchart of multiscale modeling. The magnetic field is computed by linear approximated magnetic field. The magnetization vector is computed by the magnetization vector obtained from (12).

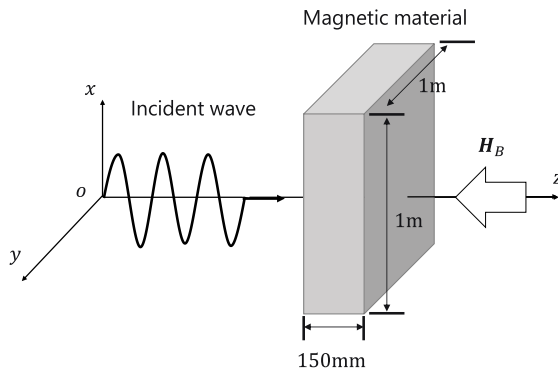


FIGURE 7. Computational model of a magnetic material with thickness 150 mm and microwave impinging. The linear polarized wave propagates to +z direction and contains x components of the magnetic field.

M_M obtained from (11) and (12): The magnetization vector was computed using the linearly approximated magnetic field H_M .

The restricted time step can be reduced by increasing the space step size for solving Maxwell's equations with respect to the space step size for solving the LLG equation. Alternatively, fine cells can be used to represent magnetic materials while maintaining the space step size to solve Maxwell's equations.

III. COMPUTATIONAL RESULTS

Fig. 7 shows the computational model. The magnetic film was placed at $z = 50\text{--}200$ mm in free space, and the incident wave was linearly polarized with only the x component of the magnetic field and frequency $f = 10$ GHz and has the waveform illustrated in Fig. 8. This electromagnetic wave is assumed to be irradiated from a waveguide to a magnetic material. The magnetic film was comprised of yttrium iron garnet. In a free space, the electromagnetic field is obtained by Maxwell's equations. In the presence of a magnetic film, the LLG equations and Maxwell's equations are solved simultaneously to obtain the magnetization and electromagnetic field.

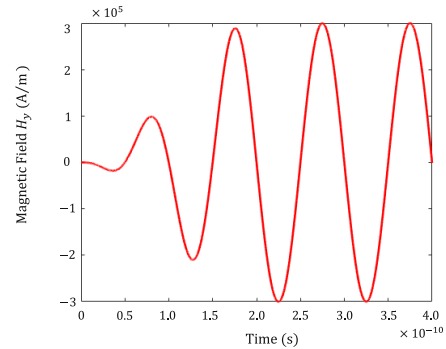


FIGURE 8. Waveform of incident plane wave.

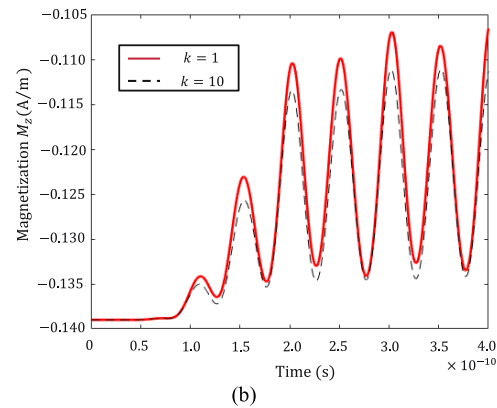
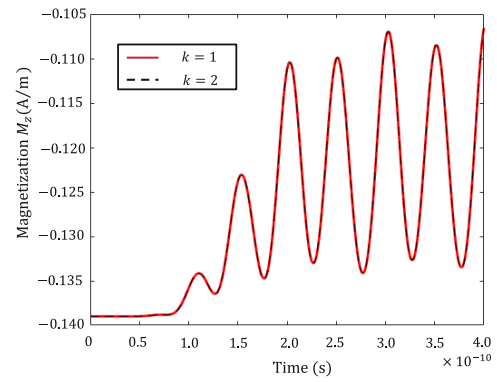


FIGURE 9. Time response waveform of magnetization compared to reference solution (a) $k = 2$, (b) $k = 10$.

The computational parameters were $\gamma = 2.21 \times 10^5$ rad/T, $\alpha = 2.3 \times 10^{-4}$, $M_s = 1.39 \times 10^5$ A/m, and $A = 4.15 \times 10^{-12}$ J/m. The magnetization in the film was in the negative z-axis direction using an external magnetic field with an amplitude $H_B = -4.76 \times 10^5$ A/m [21]. The space step size for solving the LLG equation was fixed at $\Delta x = 1$ m, $\Delta y = 1$ m, and $\Delta z = 1 \times 10^{-6}$ m. Perfectly matched layer (PML) is used as the absorbing boundary condition. The development environment in this study is as follows: Coding language: MATLAB 2023b, OS: Windows 10 Education, version: 22H2, CPU: 11th Gen Intel(R) core(TM) i7-11700@2.50GHz, memory: 64 GB.

Fig. 9 illustrates the time-response waveforms of magnetization. The red solid line is the result of the conventional

TABLE 1. Computational time and accuracy for the multiscale modeling.

k	Δz (m) (Maxwell)	Δz (m) (LLG)	Computational time (s)	Digits of accuracy
1	1×10^{-6}	1×10^{-6}	873747	—
2	2×10^{-6}	1×10^{-6}	379890	4
3	3×10^{-6}	1×10^{-6}	203673	3
10	10×10^{-6}	1×10^{-6}	52174	2

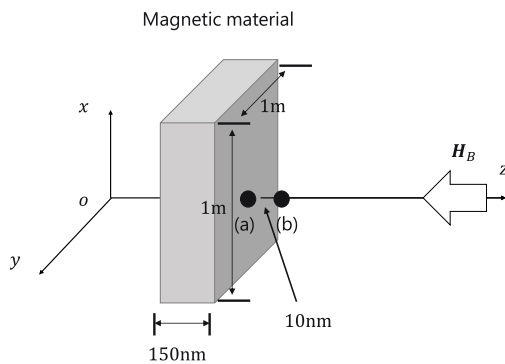


FIGURE 10. Configuration of the analysis of a 150 nm thick nanoscale magnetic film.

method ($k = 1$), and the black dotted line is the result of the multiscale modeling ($k = 2, 10$). All results obtained by the conventional multiphysics method and multiscale modeling are in agreement.

Table 1 lists the computation time and accuracy for the multiscale modeling. The analysis was performed up to a steady state $T = 0.4$ ns. The space step size for solving the LLG equation was fixed at 1×10^{-6} m. The space step size for solving Maxwell’s equation was set to discrete values: 2×10^{-6} m, 3×10^{-6} m, and 10×10^{-6} m, whereas the one for solving the LLG equation was fixed at 1×10^{-6} m. The digits of accuracy indicate the relative error when the $k = 1$ case is used as the reference solution in the proposed method, which is the same condition as the conventional method [18], [19]. When k increased, the computational time is reduced by approximately $1/k$ times. The accuracy was approximately four digits when $k = 2$, and two digits when $k = 10$. As k is increased, the accuracy of the FDTD decreases because the discretization size of the electromagnetic field increases. Comparing $k = 2$ and $k = 10$, we observe a 2-digit change in digits of accuracy. This is because the calculation accuracy of FDTD is determined by the square of the discretization size [9].

An analysis of a nanoscale magnetic film is presented as an example of the application of this method. Fig. 10 shows the computational model. The thickness of the magnetic film was 150 nm and $k = 50$. The computational cost of analyzing nano-sized magnetic models using conventional analytical

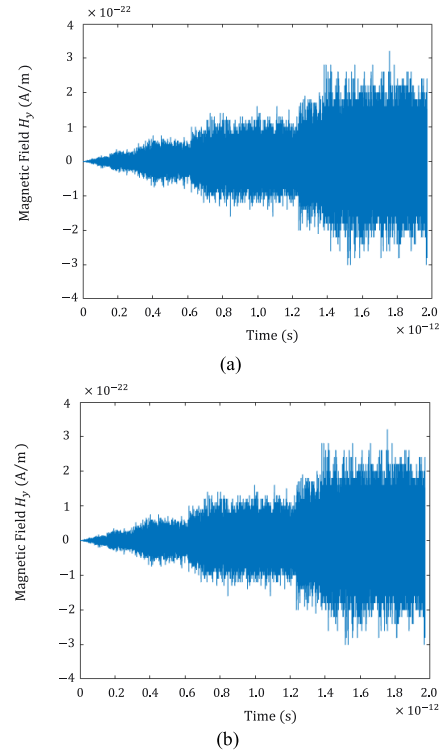


FIGURE 11. Time response waveform of magnetic field (a) in magnetic film (b) near magnetic film.

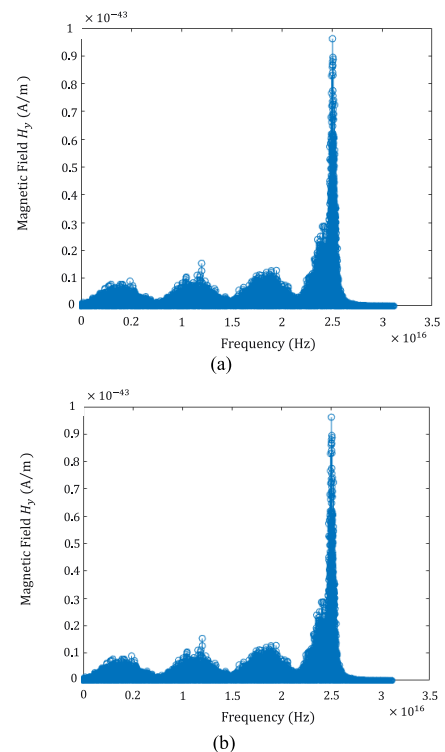


FIGURE 12. Frequency response of the magnetic field (a) in the magnetic film (b) near the magnetic film.

methods is prohibitive. The use of a multi-scaling model, which greatly reduces the computational cost, enables the

analysis of nanosized magnetic films. Fig. 11 shows the time response waveforms of the magnetic field at two observation points. The two observation points, (a) and (b), were 10 nm apart. Fig. 12 shows the frequency characteristics of the magnetic field obtained by applying the fast-Fourier-transform (FFT) [24] to the time response waveform shown in Fig. 11. Although magnetization generates standing waves inside the magnetic film, the magnetic field observed outside the magnetic film can be used to measure the nonlinearity of the magnetization and the magnetic properties from the magnetic field in the vicinity of the magnetic film. Although it was impractical to perform the analysis in terms of the analysis time using the conventional method, the multi-scaling model resulted in an analysis time of 1053508 s.

IV. CONCLUSION

This study examined multiscale modeling to reduce the computation time for multiphysics simulations of Maxwell's and LLG equations. Accordingly, the space step size of the electromagnetic field and that of the magnetization dynamics were varied to determine the relationship between the computing time and simulation accuracy. The computational time for the variable space step size was investigated, and it was found to be reduced by a factor of approximately the reciprocal of the ratio between the space step size of the electromagnetic field and that of the magnetization, that is, $1/k$. Furthermore, as an application of our method, analysis of a nanoscale magnetic film was performed. Magnetic properties can be measured using a magnetic field near the magnetic film.

REFERENCES

- [1] N. Kanazawa, T. Goto, K. Sekiguchi, A. B. Granovsky, C. A. Ross, H. Takagi, Y. Nakamura, H. Uchida, and M. Inoue, "The role of Snell's law for a magnonic majority gate," *Sci. Rep.*, vol. 7, no. 1, pp. 1–8, Aug. 2017, doi: [10.1038/s41598-017-08114-7](https://doi.org/10.1038/s41598-017-08114-7).
- [2] T. Ohkochi, H. Fujiwara, M. Kotsugi, H. Takahashi, R. Adam, A. Sekiyama, T. Nakamura, A. Tsukamoto, C. M. Schneider, H. Kuroda, E. F. Arguelles, M. Sakaue, H. Kasai, M. Tsunoda, S. Suga, and T. Kinoshita, "Optical control of magnetization dynamics in Gd–Fe–Co films with different compositions," *Appl. Phys. Exp.*, vol. 10, no. 10, Oct. 2017, Art. no. 103002, doi: [10.7567/apex.10.103002](https://doi.org/10.7567/apex.10.103002).
- [3] V. G. Harris, "Modern microwave ferrites," *IEEE Trans. Magn.*, vol. 48, no. 3, pp. 1075–1104, Mar. 2012, doi: [10.1109/TMAG.2011.2180732](https://doi.org/10.1109/TMAG.2011.2180732).
- [4] A. Slavin and V. Tiberkevich, "Nonlinear auto-oscillator theory of microwave generation by spin-polarized current," *IEEE Trans. Magn.*, vol. 45, no. 4, pp. 1875–1918, Apr. 2009, doi: [10.1109/TMAG.2008.2009935](https://doi.org/10.1109/TMAG.2008.2009935).
- [5] A. Khitun, M. Bao, and K. L. Wang, "Spin wave magnetic NanoFabric: A new approach to spin-based logic circuitry," *IEEE Trans. Magn.*, vol. 44, no. 9, pp. 2141–2152, Sep. 2008, doi: [10.1109/TMAG.2008.2000812](https://doi.org/10.1109/TMAG.2008.2000812).
- [6] H. Cui, Z. Yao, and Y. E. Wang, "Coupling electromagnetic waves to spin waves: A physics-based nonlinear circuit model for frequency-selective limiters," *IEEE Trans. Microw. Theory Techn.*, vol. 67, no. 8, pp. 3221–3229, Aug. 2019, doi: [10.1109/TMTT.2019.2918517](https://doi.org/10.1109/TMTT.2019.2918517).
- [7] J. Li, C. B. Wilson, R. Cheng, M. Lohmann, M. Kavand, W. Yuan, M. Aldosary, N. Agladze, P. Wei, M. S. Sherwin, and J. Shi, "Spin current from sub-terahertz-generated antiferromagnetic magnons," *Nature*, vol. 578, no. 7793, pp. 70–74, Feb. 2020, doi: [10.1038/s41586-020-1950-4](https://doi.org/10.1038/s41586-020-1950-4).
- [8] R. Khymyn, I. Lisenkov, V. Tiberkevich, B. A. Ivanov, and A. Slavin, "Antiferromagnetic THz-frequency josephson-like oscillator driven by spin current," *Sci. Rep.*, vol. 7, no. 1, p. 43705, Mar. 2017, doi: [10.1038/srep43705](https://doi.org/10.1038/srep43705).
- [9] A. Taflove and S. C. Hagness, *Computational Electrodynamics the Finite-Difference Time-Domain Method*. Boston, MA, USA: Artech House, 2005, p. 51.
- [10] T. Nakazawa, D. Wu, S. Kishimoto, J. Shibayama, J. Yamauchi, and S. Ohnuki, "Error-controllable scheme for the LOD-FDTD method," *IEEE J. Multiscale Multiphys. Comput. Techn.*, vol. 7, pp. 135–141, 2022, doi: [10.1109/JMMCT.2022.3181568](https://doi.org/10.1109/JMMCT.2022.3181568).
- [11] D. Wu, S. Kishimoto, and S. Ohnuki, "Optimal parallel algorithm of fast inverse Laplace transform for electromagnetic analysis," *IEEE Antennas Wireless Propag. Lett.*, vol. 19, pp. 2018–2022, 2020, doi: [10.1109/LAWP.2020.3020327](https://doi.org/10.1109/LAWP.2020.3020327).
- [12] S. Ohnuki, R. Ohnishi, D. Wu, and T. Yamaguchi, "Time-division parallel FDTD algorithm," *IEEE Photon. Technol. Lett.*, vol. 30, no. 24, pp. 2143–2146, Dec. 2018.
- [13] K. S. Kunz and R. J. Luebbers, *The Finite Difference Time Domain Method for Electromagnetics*. Boca Raton, FL, USA: CRC Press, 1993, pp. 308–322.
- [14] D. R. Smith and D. Schurig, "Electromagnetic wave propagation in media with indefinite permittivity and permeability tensors," *Phys. Rev. Lett.*, vol. 90, no. 7, Feb. 2003, Art. no. 077405, doi: [10.1103/physrevlett.90.077405](https://doi.org/10.1103/physrevlett.90.077405).
- [15] J. A. Pereda, L. A. Vielva, A. Vegas, and A. Prieto, "An extended FDTD method for the treatment of partially magnetized ferrites," *IEEE Trans. Magn.*, vol. 31, no. 3, pp. 1666–1669, May 1995, doi: [10.1109/20.376355](https://doi.org/10.1109/20.376355).
- [16] J. A. Pereda, L. A. Vielva, M. A. Solano, A. Vegas, and A. Prieto, "FDTD analysis of magnetized ferrites: Application to the calculation of dispersion characteristics of ferrite-loaded waveguides," *IEEE Trans. Microw. Theory Techn.*, vol. 43, no. 2, pp. 350–357, Feb. 1995, doi: [10.1109/22.348095](https://doi.org/10.1109/22.348095).
- [17] Z. Yao, R. U. Tok, T. Itoh, and Y. E. Wang, "A multiscale unconditionally stable time-domain (MUST) solver unifying electrodynamics and micromagnetics," *IEEE Trans. Microw. Theory Techn.*, vol. 66, no. 6, pp. 2683–2696, Jun. 2018, doi: [10.1109/TMTT.2018.2825373](https://doi.org/10.1109/TMTT.2018.2825373).
- [18] M. M. Aziz, "Sub-nanosecond electromagnetic-micromagnetic dynamic simulations using the finite-difference time-domain method," *Prog. Electromagn. Res. B*, vol. 15, pp. 1–29, 2009, doi: [10.2528/pierb09042304](https://doi.org/10.2528/pierb09042304).
- [19] M. M. Aziz and C. McKeever, "Wide-band electromagnetic wave propagation and resonance in long cobalt nanoprisms," *Phys. Rev. Appl.*, vol. 13, no. 3, Mar. 2020, Art. no. 034073, doi: [10.1103/physrevapplied.13.034073](https://doi.org/10.1103/physrevapplied.13.034073).
- [20] M. Slodička and I. Cimrák, "Numerical study of nonlinear ferromagnetic materials," *Appl. Numer. Math.*, vol. 46, no. 1, pp. 95–111, Jul. 2003, doi: [10.1016/s0168-9274\(03\)00010-2](https://doi.org/10.1016/s0168-9274(03)00010-2).
- [21] H. Yu, O. d'Allivy Kelly, V. Cros, R. Bernard, P. Bortolotti, A. Anane, F. Brandl, R. Huber, I. Stasinopoulos, and D. Grundler, "Magnetic thin-film insulator with ultra-low spin wave damping for coherent nanomagnonics," *Sci. Rep.*, vol. 4, no. 1, p. 6848, Oct. 2014, doi: [10.1038/srep06848](https://doi.org/10.1038/srep06848).
- [22] W. F. Brown, *Micromagnetics*. New York, NY, USA: Robert E. Krieger Publishing, 1978.
- [23] O. Vacus and N. Vukadinovic, "Dynamic susceptibility computations for thin magnetic films," *J. Comput. Appl. Math.*, vol. 176, no. 2, pp. 263–281, Apr. 2005, doi: [10.1016/j.cam.2004.07.016](https://doi.org/10.1016/j.cam.2004.07.016).
- [24] H. J. Nussbaumer, *Fast Fourier Transform and Convolution Algorithms*. New York, NY, USA: Springer-Verlag, 1981, pp. 80–111.



YUTA ITO was born in Tokyo, Japan, in 1999. He received the B.S. degree in electrical engineering from Nihon University, Tokyo, in 2022, where he is currently pursuing the master's degree. His research interest includes multiphysics simulation.



TAKUMI YASUDA was born in Tokyo, Japan, in 1996. He received the B.S. and M.S. degrees in electrical engineering from Nihon University, Tokyo, in 2018 and 2020, respectively. His research interest includes multiphysics simulation.



SEIYA KISHIMOTO (Member, IEEE) was born in Chiba, Japan, in 1987. He received the B.S., M.S., and Ph.D. degrees in electrical engineering from Nihon University, Tokyo, Japan, in 2009, 2011, and 2014, respectively. He was a Research Fellow with Japan Society for the Promotion of Science (JSPS), in 2013. From 2014 to 2019, he was with the Wireless System Laboratory, Research and Development Center, Toshiba Corporation, as a Research Scientist. In 2019, he joined the Department of Electrical Engineering, College of Science and Technology, Nihon University, where he is currently an Assistant Professor. His research interests include small antennas, tunable antennas, RFID, and fast solvers. He is a member of IEICE. He received the URSI GASS Young Scientist Award, in 2021.



KATSUJI NAKAGAWA (Member, IEEE) was born in Tokyo, Japan, in 1957. He received the B.S., M.S., and Ph.D. degrees in electronic engineering from Nihon University, Tokyo, in 1980, 1982, and 1993, respectively.

He was a Researcher for memory devices with NEC Corporation, from 1982 to 1989. He joined the Department of Electronic Engineering, College of Science and Technology, Nihon University, in 1989, where he is currently a Professor. His research interests include the field of magnetic materials and devices, optical devices, and memories. He was an Original Council Member of Asian Union

of Magnetics Societies, from 2008 to 2019. He was an AdCom Member of the IEEE Magnetic Society, from 2016 to 2021. He is the President of The Magnetics Society of Japan, from 2019 to 2021.



SHINICHIRO OHNUKI (Member, IEEE) was born in Tokyo, Japan, in 1968. He received the B.S., M.S., and Ph.D. degrees in electrical engineering from Nihon University, Tokyo, in 1991, 1993, and 2000, respectively. From 2000 to 2004, he was with the Center for Computational Electromagnetics and the Electromagnetics Laboratory, Department of Electrical and Computer Engineering, University of Illinois at Urbana-Champaign, as a Post-Doctoral Research Associate, and a Visiting Lecturer. In 2012, he was a Visiting Associate Professor.

He joined the Department of Electrical Engineering, College of Science and Technology, Nihon University, in 2004, where he is currently a Professor. His research interests include computational electromagnetics and multiphysics simulation. He was a recipient of the Research Fellowship Award from the Kajima Foundation Tokyo, in 2000. He was a co-recipient of the Best Paper Award from The Magnetics Society of Japan, in 2013, and the Technical Development Award from the Institute of Electrical Engineers of Japan, in 2014. He was a recipient of the Electronics Society Award from the Institute of Electronics, Information and Communication Engineers, in 2020. He has been on the Editorial Board of Progress in electromagnetics research, since 2017, and an Editorial Advisory Board of Wiley's *International Journal of Numerical Modelling: Electronic Networks, Devices and Fields*, since 2020. He served as an Associate Editor for IEEE JOURNAL ON MULTISCALE AND MULTIPHYSICS COMPUTATIONAL TECHNIQUES, from 2018 to 2020, and a Secretary for the URSI Committee Japan and the URSI Commission B, from 2017 to 2020.

...